Experimental requirements for light-induced reactions in powders investigated by time-resolved X-ray diffraction

J. Davaasambuu, P. Durand and S. Techert*

Max-Planck-Institut für Biophysikalische Chemie, Abteilung Spektroskopie und Photochemische Kinetik, Am Fassberg 11, 37077 Göttingen, Germany. E-mail: stecher@gwdg.de

A general outline of how to perform a light-excited time-resolved diffraction experiment by applying the optical pump/X-ray probe technique is given. Owing to the difference in penetration depths between the optical light (laser) pump and the X-ray probe, only specific or specially designed crystalline systems can be investigated, so special requirements have to be fulfilled concerning the sample and its compartments. A summary of the experimental conditions of optical pump/X-ray probe experiments is presented, emphasizing why the use of powder diffraction is a useful and necessary X-ray technique for this kind of experiment. The possibilities and bottlenecks of time-resolved X-ray diffraction on the picosecond time scale will be demonstrated in the powder diffraction studies of *N*,*N*-dimethylaminobenzonitrile and *N*,*N*-diisopropylaminobenzonitrile, where the photo-induced structural changes of these molecular organic systems have been studied as a function of time.

Keywords: time-resolved X-ray diffraction; optical light pump/X-ray probe methods.

1. Introduction

In a photo-induced time-resolved X-ray diffraction experiment, the photo-initiated change in intensity and/or in peak position of a Bragg reflection is studied as a function of time.

Fig. 1 summarizes the possible effects on a powder diffraction pattern with (solid line) and without (dashed line) illumination. The peak shifts are related to the translational properties of the lattice, *i.e.* the variation of the lattice constants. The unit-cell dimensions increase or decrease by heating or cooling or by pressure changes. In a typical light-induced experiment, laser illumination induces a warming up of the sample, *i.e.* an increase in the cell volume, which can be revealed by the shift of the Bragg diffraction peak positions (if the effect is significant). On the microscopic level, the propagation of acoustic modes is responsible for such modulations. Since acoustic modes propagate with speed of sound through the lattice, the time scale, on which position changes occur, strongly depends on the grain size in the powder.

However, light excitation also induces intensity variations of the Bragg reflections (Fig. 1). The intensity of the reflections is correlated with the geometry of a molecule *via* the square of the structure factor. Since geometrical changes cover the whole time scale, from femtoseconds to seconds, the intensity modulations also take place on the femtosecond to second time scale.

A chemical reaction can be initiated by a sudden rapid change in the thermodynamic properties of the environment, caused by temperature, concentration (stop-flow) or pressure jumps (Eigen, 1965). The reaction can also be started by an optical light pulse emitted from a flash lamp or from a laser. The combination of pulsed laser sources with pulsed X-ray sources, by using synchrotron X-ray radiation and/or X-rays from plasma sources, has made the application of pump–probe schemes possible. The principle of the experiment is summarized in Fig. 2. After photo-initiation of the reaction by a pulsed optical laser beam, the excited state is probed with an X-ray shot. By varying the delay between pump and probe pulse, a series of snapshots of the moving structure can be taken where each shot probes the average structure (non-excited and excited, including the dispersion of the latter) at a given time *t*. The set-up exists as a table-top system as well as at synchrotrons and it can reach time resolutions from seconds to picoseconds (synchrotron) (Bourgeois *et al.*, 1996; Schotte *et al.*, 2001) to subpicoseconds or a few hundred femtoseconds in plasma source experiments (table-top) (Rischel *et al.*, 1997; Rose-Petruck *et al.*, 1999; Siders *et al.*, 1999; Tomov *et al.*, 1999). This kind of experiment enables the monitoring of structural changes of short-living intermediates in the photocycle of a particular chemical or biological system. The advantage of a pump–probe experiment with ultrafast laser systems (over temperature-jump, pressure-jump or concentration-jump experiments) is the well defined time zero with respect to the system investigated, here the molecule. Within the first few tens to hundreds of femtoseconds the sample is *coherently* excited, giving a sharp and well defined time-zero signal from the pump-pulsed laser source. Using photoabsorption as the reaction-initiating step, it is additionally possible to gain the highest time-resolution during the experiment and to guide the reaction into one particular direction or into one particular reaction pathway. Flash lamps or continuous-wave (cw) lasers can also be used

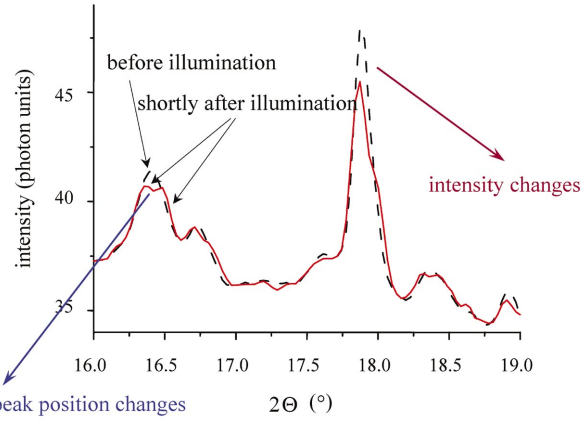

Figure 1
Possible effects of light illumination on a powder diffraction pattern.

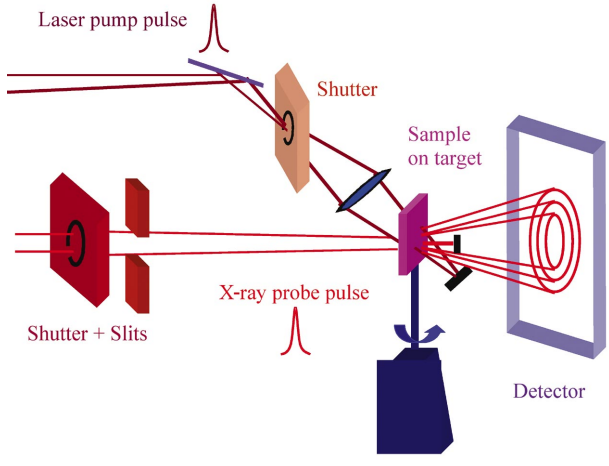

Figure 2
Principle of the optical light pump/X-ray probe set-up in time-resolved X-ray diffraction.

 doi:10.1107/S090904950402463X

to photo-initiate a reaction in particular for investigating long-living intermediates or irreversible reactions (see the following section).

The use of optical light excitation as reaction initiator has the practical advantage that the light penetrates the reaction vessel with a velocity that is proportional to the speed of light multiplied by the refraction index of the material. Therefore, one photon immediately initiates the reaction if it is absorbed by a chromophore. Rapid diffusion-controlled equilibrium processes, as they occur in temperature-jump experiments or pressure-jump experiments, are the reaction steps, which determine the kinetics of the system on a longer time scale.

In one approach for optical light pump/X-ray probe experiments, the slow time scales of a crystal reaction on light can experimentally be covered by so-called stroboscopic experiments, where the time delay between laser pump and X-ray probe is fixed so that quasi-stationary structures of transient species can be investigated. With this method, intermediates of reversible light-driven processes with microsecond lifetimes are characterized. Fig. 3 summarizes the different time scales of processes that can occur in a solid. For the diffraction mode, millisecond to microsecond time-resolved experiments were first investigated, as described by Pressprich *et al.* (1994) and Gütlich *et al.* (1994) for an X-ray laboratory source, and by Chen *et al.* (2001) using synchrotron radiation. The method is very good for measuring accurate structures of intermediates up to the microsecond time scale. On the second to millisecond time scale, thermodynamical transformations and transport reactions, as well as spin-relaxed phenomena like photo-induced ferromagnetism or ferroelectricity, can be studied. Pioneering work in this field can be found by Gütlich *et al.* (1994) and Kusz *et al.* (2000).

The nanosecond to picosecond time scales, however, are characterized by the electronic lifetimes of electronically excited singlet states and some slow relaxation processes which quench the optical response of material under light excitation (like fluorescence or phosphorescence, Fig. 3). These relaxation processes are rotational motions or vibrational motions like librations, large-amplitude motions or acoustic modes. Vibrational motions of higher frequencies dominate the femtosecond time scale.

However, two problems when investigating photo-induced processes can occur.

First, according to the Woodward–Hofman rules and depending on the symmetry of the system (Klessinger & Michl, 1989), photo-

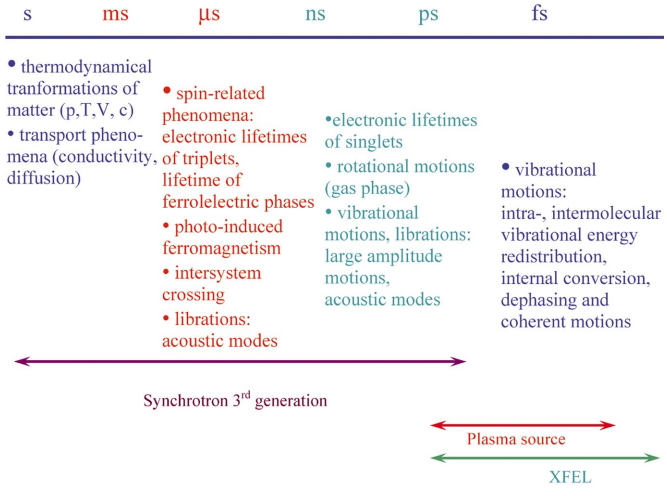

Figure 3
Time scales of molecular effects which are possible in the solid phase.

chemical and thermally initiated reaction products are exclusively formed. This can be explained by the fact that the photon has a spin of 1. Under spin and energy conservation, the product states must be different compared with heat-jump experiments. As a consequence of this general limitation, photo-induced processes might not always simulate temperature-initiated processes. The latter finding, however, is valid for the whole photochemical field, independent of the probe source used (infrared, Raman, X-ray *etc.*).

The second, more general, problem particularly concerns pump/probe schemes, where optical light is used as the pump source and X-rays are used as the probe source (or *vice versa*). This problem is caused by the fact that the cross sections of the scattered X-ray photons ($\sim 10^{-15}$ cm^2) are two orders of magnitude smaller than the cross sections of the optical photons ($\sim 10^{-13}$ cm^2). In order to reach a sufficient signal-to-noise ratio of the X-ray signals for reliable data treatment, the optical light excitation conditions and X-ray probe conditions have to be chosen in such a way that the material is photo-excited as homogeneously as possible. Working out exactly these conditions is the topic of the present paper.

In the following we will concentrate on the technical issues of investigating photoreactions. Here, the creation of intermediates follows the optical selection rules. The initiated reaction pathway is a repetitive photocycle. The lifetimes of the investigated intermediates are of the order of nanoseconds.

2. Methodology and discussion

2.1. Experimental requirements for photo-induced powder diffractometry

In this contribution we will concentrate on the technical considerations for time-resolved X-ray diffraction (TR-XRD) on single crystals or powder diffraction, where the structure factors of a system are measured as a function of time. We will mainly concentrate on the technical difficulties arising from a diffraction experiment.

In order to obtain a significant signal-to-noise ratio of the diffraction data, which would allow the treatment of the data (see the following section), at least 5% of the sample should be optically excited. As an example, the system of interest will be organic chromophores, though the general rules presented in this work can be applied to every light-absorbing system. In TR-XRD, two sets of parameters have to be optimized within and to each other so that they match best: the optical excitation conditions on the pump side and the X-ray probe characteristics. Here, one major difficulty is the geometrical overlap of the optically excited area in the crystal which should ideally be homogeneously probed by the monochromatic X-ray pulse. Fig. 4 summarizes these circumstances. In general, the optical density oD of a molecular system is defined as the product of the molar extinction coefficient ε, absorption length l and concentration c of the absorbing species. Since the oD is very high in chromophoric crystals, or in highly concentrated dyes solutions ($c \simeq 10^{-2} M$), and, when using organic molecules containing phenyl moieties (with extinction coefficients of $\varepsilon \simeq 20\,000$ mol cm^{-1}), the optical density of the material can easily reach a maximal value of oD = 4–5 for crystalline materials with a thickness $l = 100$ µm or a solution of the dye in a capillary of thickness 100 µm. Applying the Lambert–Beer law [with $I = I_o \exp(-\varepsilon c l)$], optical photons simply penetrate only a few micrometres into the crystal yielding a small non-homogeneous excitation located mainly at the surface of the crystal. The left-hand side of Fig. 4(*a*) (dotted line) shows such a low penetration of optical light owing to the high chromophore concentration in the crystal and a high extinction coefficient. In contrast (Fig. 4*b*, dotted line), reasonable X-ray probe wavelengths of $\lambda_{X\text{-ray}} =$

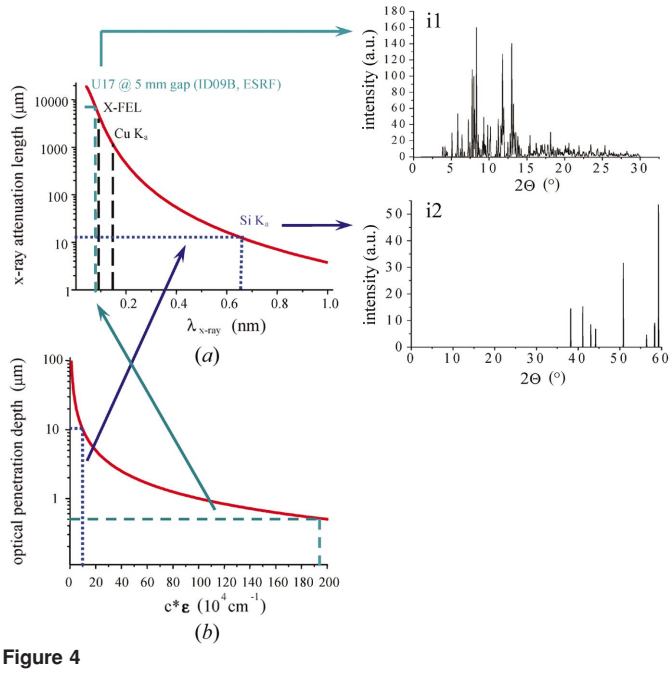

Figure 4
Difference in penetration depth for optical light pulses and X-ray probe pulses. The problem of penetration depth arises for every chromophoric system in the condensed or solid state when a critical amount of concentration of the chromophore is reached.

1–2 Å penetrate more than 100 μm into the material owing to the low X-ray cross section. According to Fig. 4, the optimal geometric match between optical light pump and X-ray probe would be reached with X-ray wavelengths of $\lambda_{X\text{-ray}}$ = 7–10 Å which are represented as dashed lines in Fig. 4(*a*) and Fig. 4(*b*). Inset i2 shows a simulation of a powder diffraction pattern for the Si K_α line at $\lambda_{X\text{-ray}}$ = 7.1 Å. The small amount of reflections is not enough for statistical relevance. They would be required for a satisfying structure refinement of a transient species with unknown geometry.

Monochromatic light selected from an in-vacuum undulator, such as U17 at the ID09 beamline of the ESRF in Grenoble, allows the collection of powder diffraction patterns to high diffraction angles (Fig. 4, inset i1). Owing to the long penetration depth of the monochromatic undulator spectrum ($\lambda_{X\text{-ray}}$ = 0.738 Å) of some hundred micrometres, and in contrast to the optical penetration depth of some micrometres, for systems with high optical extinction coefficient, it is optimal to work in the case of powders with grain sizes smaller than 1 μm rather than with single crystals in the micrometre range, which brings us to powder diffraction studies. Here, a homogeneous optical excitation is guaranteed, which can be probed by any X-ray wavelength, also allowing small wavelengths leading to high spatial resolution.

2.2. Sample preparation

For time-resolved powder diffraction, three methods for preparing powder samples turned out to be most suitable:

(*a*) Purified, recrystallized and crushed samples are pressed into a gasket with a hole in the centre. Its diameter fits the focus diameter of the laser and X-ray beam. Depending on the optical density of the chosen material and the optical excitation wavelength, the thickness of the sample should not exceed 10–50 μm. The sample can be prepared in a diamond anvil cell and be pressed until it becomes optically transparent (Fig. 5*a*).

(*b*) Organic powder can be dispersed on a substrate like mica, mylar foil or kapton foil. Alternatively, the powder can also be deposited between two substrate plates with a mask of 5–10 μm as space holder. Note that owing to its yellow appearance, kapton absorbs beyond 400 nm. The thickness of the substrate itself should not exceed 5–20 μm. Mylar and mica both have the advantage of being optically transparent (up to ∼300 nm) and give well defined spots (mica) or diffuse X-ray scattering signals (mylar) in the diffraction pattern, which can be masked out or compensated (Fig. 5*b*).

(*c*) As an alternative method, growing the chromophore in a host matrix might be considered (Coppens *et al.*, 2002). Though technically more demanding than the preparation methods suggested in this work, embedding the chromophore in a host lattice gives an alternative possibility of homogeneous optical excitation even in single crystals.

2.3. Optical excitation of powders

Fig. 6 compares the optical spectra of *N*,*N*-diisopropylaminobenzonitrile (DIABN) powder prepared on the different substrates as described above. The structure of DIABN is shown in the inset in Fig. 6. The solid line represents the absorption spectrum of crystalline DIABN dispersed in a KBr pellet. This method is commonly used as a preparation method to characterize the optical spectra of crystalline organic matter. The dash-dotted spectrum represents DIABN crystallites dispersed on mylar and the dashed spectrum represents DIABN on quartz. The DIABN spectrum on mylar is shown only to demonstrate the increase of absorbance of the mylar, which strongly disturbs the absorption spectrum of DIABN. The absorption spectrum of DIABN on quartz is comparable with that of DIABN on KBr. The optical density does not exceed 0.3, and the thickness of the

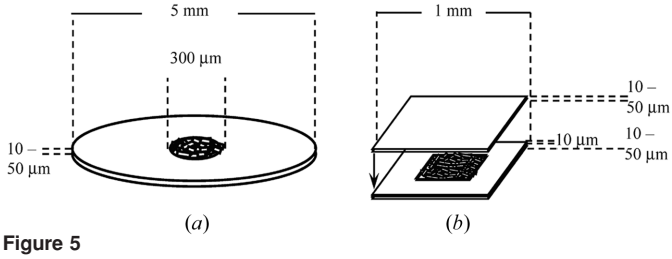

Figure 5
Typical types and dimensions of sample compartments for TR-XRD.

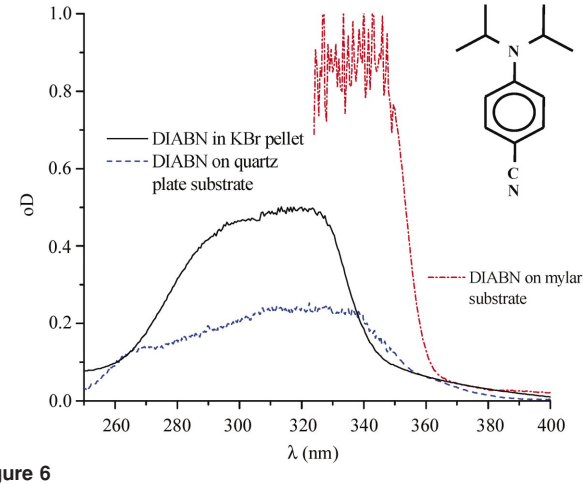

Figure 6
Optical spectra of DIABN (structure in inset) on different substrates.

chromophore layer on quartz is of the order of 5 µm. Actually, in order to create the most uniform light excitation in the sample, the oD should range between 0.5 and 1, guaranteeing an excitation yield of about 99.8% over the whole powder sample range of 5–10 µm. The absorption band of the pure powder on the quartz plate is slightly broader than the spectrum in the KBr pellet. This might be explained by an increase of excitation of optical phonons which leads to a broadening of the absorption spectrum.

2.4. Experimental set-up

The experimental set-up referred to in this work has been built at the ID09B beamline of the ESRF. The use of the set-up for TR-XRD has been extensively reported in several publications. Therefore only a few key parameters of the beamline are given here.

The time-resolved set-up at ID09B follows a classical optical pump/X-ray probe scheme as explained elsewhere (Schotte *et al.*, 2001). The pump wavelength of the mode-locked Ti:sapphire laser, which runs synchronously with single pulses of the X-rays (probe), was generated by frequency tripling to $\lambda_{exc} = 267$ nm. This excitation wavelength has been used for organic systems like *N*,*N*-dimethylaminobenzonitrile (DMABN) and DIABN. The pulse width of the laser was around 300 fs. The laser beam was focused down to a diameter of 200–400 µm. The laser power and focus have been adjusted to show no ablation or photochemical degradation effects. The X-ray probe pulses were selected from the 16-bunch filling mode of the storage ring using a synchronized chopper. For a pulse width of 70 ps (X-ray), a flux on the sample of 0.5×10^8 to 2×10^8 photons s^{-1} $(100\ mA)^{-1}$ $(0.01\%\ bandwidth)^{-1}$ was obtained in a 200 µm × 200 µm focal spot. The monochromatic X-ray probe beam at 16.5 keV ($\lambda_{X\text{-}ray} = 0.753$ Å) was selected by a Si(111) monochromator (DIABN). Note that in the case of DMABN, $\lambda_{X\text{-}ray} = 1.325$ Å was used (Techert *et al.*, 2001). Diffraction data were collected with a MAR133 CCD camera (diameter = 133 mm, pixel size = 64.7 µm × 64.7 µm), varying sample-to-detector distances of 120–160 mm depending on the desired resolution of the powder diffraction pattern. The exposure time was 10 min. During the measurements, the decay of the storage-ring current was monitored online and later included in the intensity correction of the diffraction pattern. The laser and X-ray beams hit the sample in a quasi-parallel configuration resulting in an optimal overlap between pump and probe volume.

At the beginning of a measurement cycle, time zero ($t = 0$) was set by monitoring the pulse sequence of the direct laser and the X-ray beam by using a fast GaAs detector. For negative times ($t_i < 0$), the X-ray pulse arrives before the laser pulse, whereas for positive times the X-ray pulse arrives after the laser pulse. The time-zero setting was accurate within 30 ps [jitter (X-ray laser pulse) = 3 ps]. The repetition frequency of the stroboscopic experiment was 897 Hz.

The XRD experiments were carried out at room temperature. Further experimental details can be found by Techert *et al.* (2001) and Techert & Zachariasse (2004).

2.5. Assumptions for the powder data processing

In a system, which is prepared in such a way, it is assumed that the sample is most homogeneously excited and that the number of excited chromophores is statistically distributed over the whole lattice. Fig. 7 illustrates such a statistical excitation of the sample, where the light-induced structural changes create local non-periodical perturbations in the crystal lattice. Note that the *position* of the asymmetric units in the unit cell is fixed so that the periodicity and symmetry of the lattice remains the same. Assuming that every absorbed chromophore centre causes a centre of structural defect (the molecule which has absorbed a photon reacts by structural rearrangements), and depending on the excitation wavelength and the number of exciting photons, three excitation extremes are possible:

(i) $\alpha_{abs} N^m = N_{ph}^{abs} = N_{molec}^{refined}$. The number of absorbed optical photons, N_{ph}^{abs}, is the product of the molecular absorption coefficient α_{abs} multiplied by the number of molecules in the crystal lattice (N^m). It can be estimated by the intensity of the absorbed light by applying the Lambert–Beer law or determining the extinction coefficient. Both quantities are proportional to the molecular absorption coefficient α_{abs}.

The number of absorbed optical photons N_{ph}^{abs} is equal to the number of 'defect' molecules, *i.e.* $N_{ph}^{abs} = N_{molec}^{refined}$. Since the light-induced structural changes do not lead to a formation of new domains in the lattice, the local disorder can be treated as structural defects: the representative cell is statistically populated, which expresses the probability that a certain site will be occupied by a given atom, which is $N_{molec}^{refined}$. The local disorder is created when the molecules react on the absorption of light by structural rearrangements (= N_{ph}^{abs}). The compound is then better defined by a crystallochemical formula which takes into account its occupancy in a given crystallographic site. The treatment of photo-induced effects is then rather similar to considerations of defect structures in, for example, the spinel/inverse-spinel system. The number of these defect centres is $N_{molec}^{refined}$.

In the case of $N_{ph}^{abs} = N_{molec}^{refined}$, the structural disorder refined is *localized* on molecular units in the crystal lattice, which have absorbed an optical photon. TR-XRD here probes *intramolecular* energy-dissipation processes in which localized molecular modes are involved (in the form of 'Frenkel excitons', *e.g.* if electronic transitions are involved). Two examples of this kind of excitations are refined here, in TR-XRD studies of DMABN and DIABN.

(ii) $N_{ph}^{abs} >> N_{molec}^{refined}$. If the number of absorbed photons exceeds the number of refined defect centres, the structural relaxation from the disturbed structure might be much faster than the time-resolution of the apparatus.

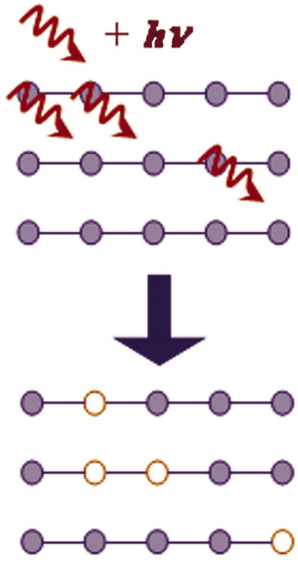

Figure 7
Schematical presentation of statistical excitations of chromophores in a crystal lattice. The lattice points which have been photo-excited are shown as opened circles.

(iii) $N_{ph}^{abs} < N_{molec}^{refined}$. If the number of absorbed photons is much smaller than the number of refined defect centres, one photon initiates the transformation of a whole cascade of molecules which can be described as a *cooperative process*. In these processes the energy dissipation progresses *intermolecular via* the formation of so-called strings. In terms of energy it means the activation of phonons migrating through the lattice (*e.g.* as low-frequency modes) or the excitation of excitons if an electronic transition is involved. An example of the latter is demonstrated by Collet *et al.* (2003).

2.6. One-dimensional powder diffraction pattern

In the following we will concentrate on the treatment of the experimental data, where the number of absorbed optical photons is equal to the number of refined 'defect molecules' [case (i) above]. Fig. 8 shows the Rietveld refinement of a powder pattern of DMABN, 80 ps after light-excitation (top), and the refinement of the 60 ps time point of light-excited DIABN powder. The corresponding experiments were performed at the ID09B beamline of the ESRF. The two-dimensional data accumulated on a CCD detector (MAR 133) were integrated using the program *Fit2d* (Hammersley *et al.*, 1996). Within the framework described in this work, the powder diffraction patterns were analysed and the structures refined by applying the Rietveld method (Rietveld, 1969; McCusker *et al.*, 1999) [using the *GSAS* program package (Larson & Von Dreele, 2000) within the *EXPGUI* interface (Toby, 2001), or the reflex software in the *MSI* software package (Reflex-Plus, 2002)].

Fig. 8(*a*) presents the diffraction pattern of DMABN during the process of refinement. The actual R_{wp} value of the pattern shown was $R_{wp} = 11\%$. Fig. 8(*b*) shows the powder diffraction pattern of DIABN after a successful refinement ($R_{wp} = 5.8\%$). Both patterns belong to an early time point after photo-initiation (DMABN, 80 ps; DIABN, 60 ps). The sharpness of the diffraction peaks at reasonable resolution of the data (note that $\lambda_{X\text{-}ray} = 1.325$ Å and $\lambda_{X\text{-}ray} = 0.753$ Å) verifies the quality of the sample, which is not affected by the preparation method or optical measurements.

In order to derive the time course of a reaction, the investigated structural changes have to be evolved as a *function of time*, preferably as *correlation functions*. Details concerning this topic can be found by Techert & Zachariasse (2004) and will not be reviewed here. Detailed descriptions of the photo-physics of the systems and the effects found are summarized by Techert *et al.* (2001), Techert & Zachariasse (2004) and Techert (2004).

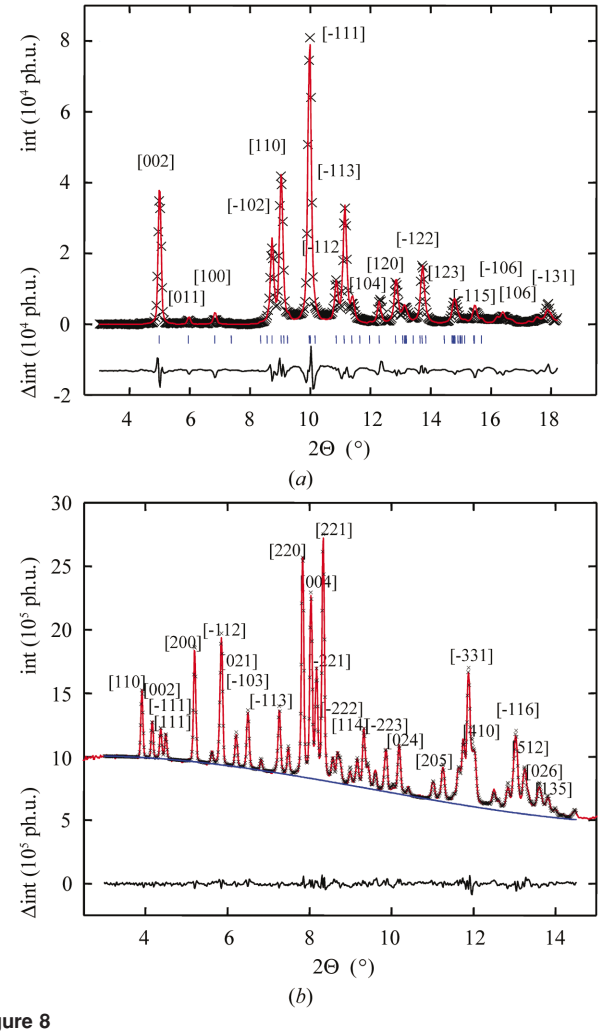

Figure 8
(*a*) Rietveld refinement of light-excited DMABN (80 ps time point, during the rigid-body refinement with $R_{wp} = 11\%$, $\chi^2 = 3.52$, $R_{exp} = 10.24\%$, $\lambda_{X\text{-}ray} = 1.325$ Å). (*b*) Converged Rietveld refinement of light-excited DIABN after rigid-body refinement (60 ps time point, $R_{wp} = 5.8\%$, $\chi^2 = 5.6$, $R_{exp} = 0.98\%$, $\lambda_{X\text{-}ray} = 0.753$ Å).

2.7. Artefacts of TR-XRD experiments

In the following, two possible artefacts for powder samples upon photo-excitation will be discussed: sample heating and possible photo-induced preferred orientation. Experimental approximations will be presented in order to estimate the extent of photo-induced side effects.

2.7.1. Heating of the sample upon optical excitation and radiation damage. The overall heating of the sample could be determined from the 2Θ shift of the Bragg diffraction peak maxima by comparing the diffraction pattern under light illumination with the dark diffraction pattern. In the samples presented in this paper, the overall heating of the sample was found to be negligible. Fig. 9 presents the difference map for DMABN (Fig. 9*a*) and DIABN (Fig. 9*b*). The intensities of the difference signal, Δint, of the photo-excited states of DMABN and DIABN are obtained by subtracting the intensities of the partially excited crystalline material from those of the non-excited powder in the electronic ground state. To do so, the data for $t = \infty$ were recorded at a time when the laser arrived just after the X-rays ($t = -120$ ps for DMABN and $t = -150$ ps for DIABN). These data were compared with those at positive times, at which the laser pulse arrived just before the X-rays, here 80 ps (DMABN) and 60 ps (DIABN) after optical excitation. After laser excitation, the diffraction signal originates from a mixture of ground-state molecules and excited-state molecules. However, in the difference map, the non-excited molecules in the unit cells do not contribute to the difference signal. The plot of intensity difference maps can give some kind of first indication, whether the photo-induced processes in the crystals or powder are heating artefacts leading to photo-degradation of the samples. The most prominent Bragg reflection changes in Figs. 9(*a*) and 9(*b*) are marked by their Miller indices *hkl*. The intensity changes range between 1% and 20% in the case of DMABN, and between 1% and 8% of the total signal in the case of DIABN. The difference in the signal change is due to the lower optical excitation in the case of DIABN (5% in contrast to around 20% in the case of DMABN). Furthermore, the photo-induced structural reorganization is smaller in the case of DMABN than in the case of DIABN (Techert *et al.*, 2001; Techert & Zachariasse, 2004). The fact that these intensity changes take place in the positive as well as in the negative direction shows that the effects observed in the present experiments are not

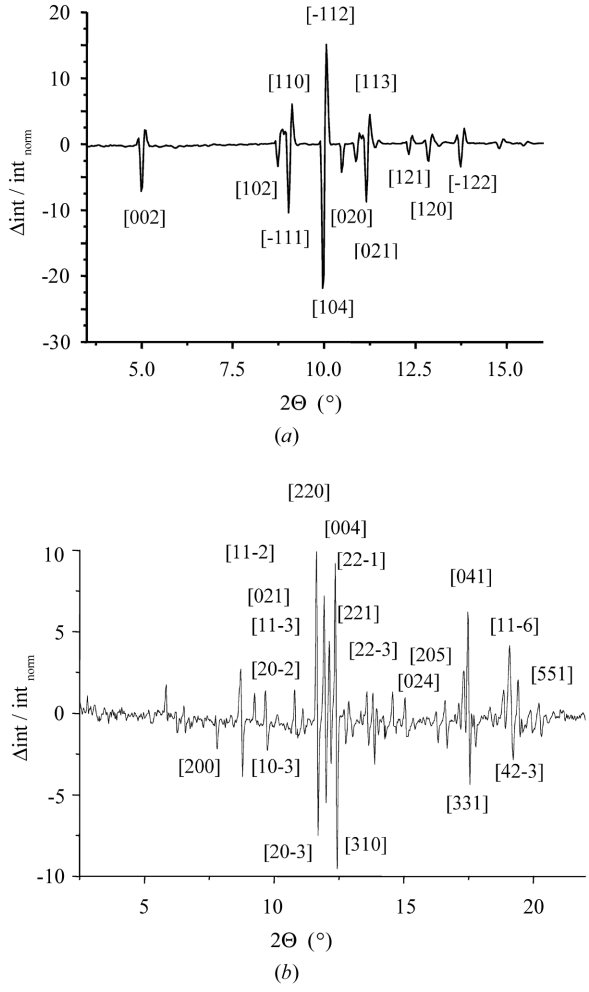

Figure 9
(*a*) Difference map of the DMABN powder spectra [80 ps − (−120 ps)]. (*b*) Difference map of the DIABN powder spectra [60 ps − (−150 ps)]. The negative time points present the time for $t = \infty$.

due to sample heating. In such a case, the intensity differences would only be negative, owing to an increase in the peak width resulting (in the most simple case) from an increase in the Debye–Waller factor. The difference map also shows that radiation damage, such as the increase of amorphous background or the gradual decrease of diffraction amplitudes, was not observed and hence does not take place, notwithstanding the repetition frequency of the experiment of 897 Hz.

2.7.2. Photo-induced preferred orientation. Owing to the way in which the samples are prepared, the occurrence of preferred orientation has to be considered and to be checked by a separate experiment. Preferred orientation of the prepared sample can be estimated or ideally excluded by comparing the intensity distribution of the various Bragg peaks of the microcrystal samples on the several substrates with powder samples in rotated capillaries. Here, the microcrystals are assumed to be randomly orientated. In the systems reported, preferred orientation was not found. To support this, with the inclusion of a preferred orientation model (March–Dollase correction), the refinement of the data has yielded R_{wp} values of between 4 and 8% without real significant improvements. The behaviour found is contrary to the scientific results obtained in pressure-dependent powder diffraction experiments on DMABN and DIABN (using a diamond anvil cell with an iron gasket). A strong effect of preferred orientation was found, which could be refined by applying the March–Dollase model in the *GSAS* package (Larson & Von Dreele, 2000) within the *EXPGUI* interface (Toby, 2001; Techert & Hanfland, 2004).

3. Summary

The optical light (laser) pump/X-ray probe technique is a very powerful method for performing time-resolved diffraction experiments with highest time resolution. Nonetheless, this method is also limited: one of the bottlenecks of the experiment is the intrinsic difference in the penetration depth between optical pump light and X-ray probe light, and special conditions concerning the preparation of the sample and the dimensions of the sample compartment have to be fulfilled. For a homogeneous sample excitation, and to compensate for the difference in penetration depth, as a general rule, the optical density of the material should not exceed oD = 1.5; ideally oD = 0.5. The latter is reached by using appropriately small grains. In this publication we have worked out the experimental requirements for performing a light-excited time-resolved diffraction experiment. We have presented the general physical background concerning TR-XRD measurements on powders, and ways of overcoming the limitations given by the optical pump/X-ray probe method.

The time-resolved X-ray diffraction experiments referred to in this work were measured at the time-resolved beamline ID09B of the ESRF. In this context, the author wishes to thank Professor Dr M. Wulff for his support of this work. Professor J. Troe is thanked for his permanent interest in this work. JD and ST are grateful to the DFG for the research grant TE/3471-2, and PD is grateful to the EU (FLASH 04). Furthermore, the Aventis Foundation is thanked for the Karl Winnacker Fellowship.

References

Bourgeois, D., Ursby, T., Wulff, M., Pradevand, C., Srajer, V., LeGrand, A., Schildkamp, W., Laboure, S., Rubin, C., Teng, T.-Y., Roth, M. & Moffat, K. (1996). *J. Synchrotron Rad.* **3**, 65–74.
Chen, L. X., Jäger, W. J. H., Jennings, G., Gosztola, D. J., Munkholm, A. & Hessler, J. P. (2001). *Science*, **292**, 262–264.
Collet, E., Lemée-Cailleau, M.-H., Buron-Le Cointe, M., Cailleau, H., Wulff, M., Luty, T., Koshihara, S.-Y., Meyer, M., Toupet, L. Rabiller, P. & Techert, S. (2003). *Science*, **300**, 612–615.
Coppens, P., Ma, B., Gerlitz, O., Zhang, Y. & Kulshretha, P. (2002). *Cryst. Eng. Comm.* **4**, 302–309.
Eigen, M. (1965). *Chem. Ber.* **98**, 1623–1628.
Gütlich, P., Hauser, A. & Spierling, H. (1994). *Angew. Chem. Int. Ed.* **33**, 2024–2054.
Hammersley, A. P., Svensson, M., Hanfland, M., Fitch, A. N. & Haeussermann, D. (1996). *High Press. Res.* **14**, 235–248.
Klessinger, M. & Michl, J. (1989). *Lichtabsorption und Photochemie organischer Molekuele.* VCH, Weinheim.
Kusz, J., Spiering, H. & Gütlich, P. (2000). *J. Appl. Cryst.* **33**, 201–205.
Larson, A. C. & Von Dreele, R. B. (2000). *GSAS General Structure Analysis System*, *Program and Handbook*. Los Alamos National Laboratory Report LAUR 86-748. University of California, USA.
McCusker, L. B., Von Dreele, R. B., Cox, D. E., Louer, D. & Scardi, P. (1999). *J. Appl. Cryst.* **32**, 36–50.
Pressprich, M. R., White, M. A., Vekhter, Y. & Coppens, P. (1994). *J. Am. Chem. Soc.* **116**, 5233–5238.
Reflex-Plus (2002). *Reflex/Reflex-Plus, MaterialsStudio.* Version 2.2, Program and Handbook. San Diego, CA: Accelrys.
Rietveld, H. (1969). *J. Appl. Cryst.* **2**, 65–71.

Rischel, C., Rousse, A., Uschmann, I., Albouy, P.-A., Geindre, J.-P., Audebert, P., Gauthier, J.-C., Förster, E., Martin, J.-L. & Antonetti, A. (1997). *Nature (London)*, **390**, 490–492.
Rose-Petruck, C., Jimenez, R., Guo, T., Cavalleri, A., Siders, C. W., Raksi, F., Squier, J. A., Walker, B. C., Wilson, K. R. & Barty, C. P. J. (1999). *Nature (London)*, **398**, 310–312.
Schotte, F., Techert, S., Anfinrud, P., Srajer, V., Moffat, K. & Wulff, M. (2001). *Picosecond Structural Studies using Pulsed Synchrotron Radiation*, in *Third-Generation Hard X-ray Synchrotron Radiation Sources*, p. 345, edited by D. M. Mills. New York: Wiley and Sons.
Siders, C. W., Cavalleri, A., Sokolowski-Tinten, K., Toth, Cs., Guo, T., Kammler, M., Horn, M., von Hoegen, M., Wilson, K. R., von der Linde, D. & Barty, C. P. J. (1999). *Science*, **286**, 1340.
Techert, S. (2004). *J. Appl. Cryst.* **37**, 445–450.
Techert, S. & Hanfland, M. (2004). In preparation.
Techert, S., Schotte, F. & Wulff, M. (2001). *Phys. Rev. Lett.* **86**, 2030–2034.
Techert, S. & Zachariasse, K. (2004). *J. Am. Chem. Soc.* **126**, 5593–5600.
Toby, B. H. (2001). *J. Appl. Cryst.* **34**, 210–213.
Tomov, I. V., Oulianov, A., Chen, P. & Rentzepis, P. M. (1999). *J. Phys. Chem. B*, **103**, 7081–7090.

 Received 1 June 2004 • Accepted 30 September 2004